Structural Engineering and Mechanics, Vol. 46, No. 1 (2013) 91-110
DOI: http://dx.doi.org/10.12989/sem.2013.46.1.091

Automated nonlinear design of reinforced concrete D regions

Hamidreza Amini Najafian and Robert L. Vollum*

Department of Civil and Environmental Engineering, Imperial College London, London SW7 2AZ, UK

(Received August 13, 2012, Revised January 12, 2013, Accepted March 6, 2013)

Abstract. This paper proposes a novel iterative procedure for the design of planar reinforced concrete structures in which the reinforcement is designed for stresses calculated in a nonlinear finite element analysis. The procedure is intended as an alternative to strut and tie modeling for the design of complex structures like deep beams with openings. Practical reinforcement arrangements are achieved by grouping the reinforcement into user defined horizontal and vertical bands. Two alternative strategies are proposed for designing the reinforcement which are designated A and B. Design constraints are specified in terms of permissible stresses and strains in the reinforcement and strains in the concrete. A case study of a deep beam with an opening is presented to illustrate the method. Comparisons are made between design strategies A and B of which B is shown to be most efficient. The resulting reinforcement weights are also shown to compare favorably with those previously reported in the literature.

Keywords: reinforced concrete; D regions; automated design of reinforcement; nonlinear analysis; plane stress; strut and tie modeling

1. Introduction

Schlaich *et al.* (1987) showed that it is convenient to divide concrete structures into B (Bernoulli) regions where plane sections remain plane after loading and D (Disturbed) regions where the strain distribution is nonlinear. D regions occur at discontinuities in loading or geometry with deep beams and squat shear walls being typical examples. The design of B regions is well covered in design standards but the design of D regions is less straightforward due its ad hoc nature. D regions are typically designed on the basis of elastic stress fields or simplified strut and tie models.

Strut and tie modeling (STM) is a generalization of the truss analogy in which a continuous structure is transformed into a discrete truss model with compressive forces being resisted by concrete and tensile forces by reinforcement. Considerable guidance is available on the development of STM (BSI 2004, fib 2011, CSA 2004, ACI 2011, ACI-ASCE 2010) but despite this it is often far from straightforward to develop a solution that is acceptable at the serviceability limit state (SLS) as well as the ultimate limit state (ULS) (Kuchma *et al.* 2010 and Hong *et al.* 2011). Various attempts have been made to automate the development of STM of which (Perera and Vique 2009, Kwak and Noh 2006, Tjhin and Kuchma 2002) are typical. All these procedures are hampered by the fact that concrete structures form a continuum rather than a set of bars as

*Corresponding author, Ph.D., E-mail: r.vollum@imperial.ac.uk

assumed in the STM (Fernández Ruiz and Muttoni 2007). Kuchma *et al.* (2010) have shown that NLFEA is a useful tool for assessing and improving the behaviour of structures designed with STM. Park *et al*. (2012) have recently formalized this procedure by developing "*an integrated design and computational framework in which a complex region first can be designed within a graphical environment by the strut-and-tie method; then its behavior can be predicted by automated nonlinear finite element analysis*".

Surprisingly, very few procedures are reported in the literature for the automated design of reinforcement in D regions using nonlinear finite element analysis. The earliest work appears to be that of Tabatabai (1996) and later Tabatabai and Mosalam (2001) who developed a computational platform for optimizing the reinforcement design in planar structures. The method finds the minimum amount of reinforcement required to resist generalized stresses calculated in an elastic finite element analysis. The minimization is performed by superimposing a series of self-equilibrating stress states on the linear elastic solution. A linear programming tableau is established in which a linear objective function is minimized whilst fulfilling a set of prescribed linear constraints. The resulting reinforcement designs are assessed with nonlinear finite element analysis following which the design constraints are checked manually. If the design constraints are not satisfied, the reinforcement field layout is changed manually and the reinforcement optimization process is repeated.

More recently, Fernández Ruiz and Muttoni (2007) developed a semi-automated approach for developing stress fields using the finite element method. Concrete is modeled as elastic-perfectly plastic in compression with no tensile resistance. Reinforcement is modeled as linearly elastic in the initial NLFEA and subsequently as elasto-plastic with strain hardening. The initial reinforcement arrangement is orthogonal with minimal reinforcement provided in each direction or based on the users' experience. Subsequently, the FE results are used to develop a stress field and the reinforcement area is recalculated in each element as $A_s = A_{s\min}\sigma_s / f_{yd} \geq A_{s\min}$ where σ_s is the reinforcement stress from the FEA, and f_{yd} is the design yield strength of the reinforcement. The final step involves manually revising the reinforcement areas and carrying out a new FEA with bilinear reinforcement to assess the overall performance of the structure.

The lack of compatibility between the assumptions made in the reinforcement design and the subsequent NLFEA means that the design constraints can only be satisfied by trial and error in both the approaches discussed above (Tabatabai and Mosalam 2001, Fernández Ruiz and Muttoni 2007). It is also notable that neither method accounts for the influence of tension stiffening on the reinforcement design. Both these issues are addressed in the current work.

2. Proposed design procedure

The proposed method is suitable for structures which can be modeled with plane stress elements using embedded grids of reinforcement. All the elements are assumed to be reinforced with orthogonal grids of reinforcement that are perfectly bonded to the surrounding concrete which is not the case in reality. Therefore, care should be taken in the detailing of the reinforcement to ensure that it is sufficiently anchored for the calculated bar forces to develop. Consequently, the NLFEA is unable to model failures resulting from inadequate anchorage of the reinforcement. The objective is to develop a safe, serviceable and practical design rather than an absolute minimum weight design. The reinforcement is designed to resist the stresses calculated in a NLFEA. Significantly, the same constitutive relationships are used in the reinforcement design as well as

Table 1 Equations of the modified compression field theory

Equilibrium	**Strain compatibility**
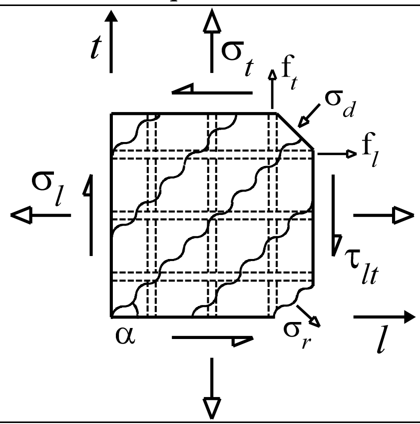	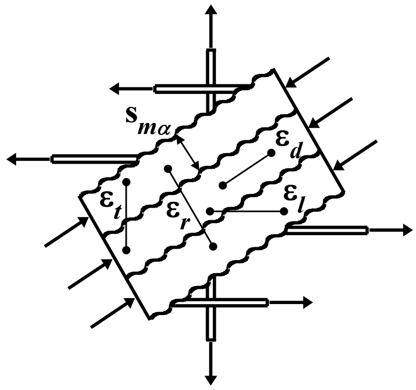
Average stresses	**Average strains**
$\sigma_l = \sigma_d \cos^2\alpha + \sigma_r \sin^2\alpha + \rho_l f_l$ (1) $\sigma_t = \sigma_d \sin^2\alpha + \sigma_r \cos^2\alpha + \rho_t f_t$ (2) $\tau_{lt} = (-\sigma_d + \sigma_r)\sin\alpha\cos\alpha$ (3)	$\varepsilon_l = \varepsilon_d \cos^2\alpha + \varepsilon_r \sin^2\alpha$ (6) $\varepsilon_t = \varepsilon_d \sin^2\alpha + \varepsilon_r \cos^2\alpha$ (7) $\gamma_{lt}/2 = (-\varepsilon_d + \varepsilon_r)\sin\alpha\cos\alpha$ (8)
Stresses at crack	**Crack widths**
$f_{slcr} = (\sigma_l + \tau_{lt}\cot\alpha - v_{ci}\cot\alpha)/\rho_l$ (4) $f_{stcr} = (\sigma_t + \tau_{lt}\tan\alpha + v_{ci}\tan\alpha)/\rho_t$ (5)	$w = \varepsilon_r s_{m\alpha}$ (9) $s_{m\alpha} = \dfrac{1}{\dfrac{\lvert\sin\alpha\rvert}{s_l} + \dfrac{\lvert\cos\alpha\rvert}{s_t}}$ (10)
Material **Reinforcement**	
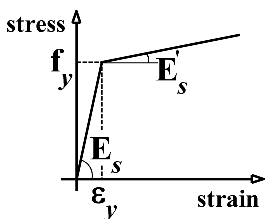	$f_l = f_l(\varepsilon_l)$ (11) $f_t = f_t(\varepsilon_t)$ (12)
Concrete	
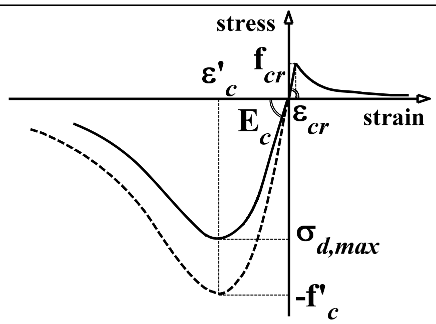	$\sigma_d = \sigma_d(\varepsilon_d, \beta)$ (13) $\sigma_r = \sigma_r(\varepsilon_r)$ (14) **Shear stress on crack** $v_{ci\max} = \dfrac{0.18\sqrt{f'_c}}{0.31 + 24w/(a+16)}$ (15)

the subsequent assessment with NLFEA. This allows explicit performance based design constraints, such as crack widths, to be specified at the design stage unlike the other procedures discussed in this paper (Tabatabai and Mosalam 2001, Fernández Ruiz and Muttoni 2007). Currently, the procedure incorporates the constitutive relations of the modified compression field theory (MCFT) (Vecchio and Collins 1986, Collins *et al*. 2008) (see Table 1) but other constitutive relationships could be used. Eqs. (1)-(3) and (6)-(8) in Table 1 are presented in the form used by Hsu (1993) and are equivalent to the corresponding equations of the MCFT. Eqs. (4)-(5) and (15) are unique to the MCFT. The Poisson's ratio for concrete is taken as zero in the NLFEA as assumed in the MCFT (Vecchio 1990).

The reinforcement design is rationalized by grouping the finite elements into horizontal (HB) and vertical (VB) bands as shown in Fig. 1. Elements at the intersection of a HB and VB bunch constitute a VHB bunch. For example, VHB1 in Fig. 1 is defined by the intersection of VB1 and HB1 which includes elements 1, 2, 13 and 14. The reinforcement ratios in the HB and VB define the reinforcement throughout the structure. The total weight of reinforcement in a VHB with surface area A is proportional to $(\rho_l + \rho_t)A$ in which ρ_l and ρ_t are the reinforcement ratios in the l and t directions respectively. It follows that the reinforcement weight is minimized in each VHB by finding the minimum value of $\rho_l + \rho_t$ that satisfies the design constraints. The reinforcement is designed in NonOpt (Amini Najafian 2011) which is a computer program developed by the authors that works in conjunction with the finite element program DIANA (2007). The entire design procedure is automated apart from the definition of the HB and VB.

2.1 Design constraints and definition of safety factors

Design constraints can be specified at either the serviceability (SLS) or the ultimate (ULS) limit state. The constraints are expressed in terms of permissible stresses in the reinforcement at cracks, principal strains in the concrete and mean strains in the reinforcement. The reinforcement ratios are also limited to $\rho_{\min}$ and $\rho_{\max}$ in accordance with the recommendations of structural codes.

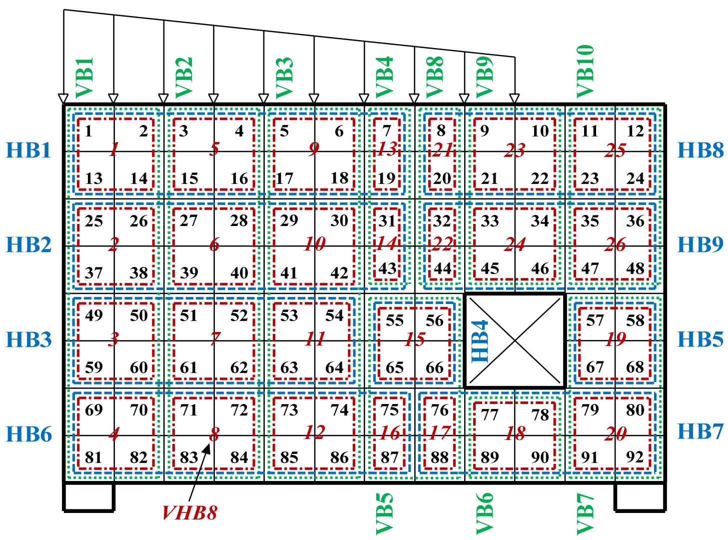

Fig. 1 Definition of VB, HB and VHB bunches in a finite element model

Limiting the principal tensile strain (ε_r) in the concrete controls the maximum crack width as well as the reduction in concrete compressive strength due to softening. Safety factors are defined for each design constraint as the ratio of the permissible strain to the actual strain. For example, the safety factor for the principal tensile strain is defined as $\varepsilon_{r,per}/\ \varepsilon_r$ where $\varepsilon_{r,per}$ is the maximum permissible principal tensile strain. The design constraints only are satisfied if all the safety factors are greater than or equal to one. The overall safety factor of a VHB is taken as the least of the safety factors calculated for each design constraint.

2.1.1 Permissible concrete strains

The maximum compressive stress in the concrete is limited by specifying a maximum permissible principal compressive strain, $\varepsilon_{d,per}$ as shown in Fig. 2. Crack widths can be controlled at either the SLS or ULS by specifying a maximum permissible principal tensile strain, $\varepsilon_{r,per}$, as follows

$$\varepsilon_{r,per} = \frac{w_{\max}}{s_{m\alpha}} \tag{16}$$

where $w_{\max}$ is the maximum permissible crack width, s_{ma} is the average spacing of cracks oriented at an angle α to the l axis which in turn depends on s_l and s_t, which are the average crack spacings normal to the l and t reinforcement respectively, as described by Eq. (10) in Table 1. The crack spacing s_l is defined (Bentz 2000) as

$$s_l = 2c + 0.1\frac{d_b}{\rho'} \tag{17}$$

in which $c = \sqrt{\mathrm{cov}^2 + (s/2)^2}$ is the diagonal distance to the closest l reinforcement bar, d_b is the reinforcement bar diameter, cov is the cover and s is the spacing of the l reinforcement. The coefficient ρ' is the reinforcement ratio of the closest l reinforcement bar within the effective concrete area A_{cef} shown in Fig. 3. The crack spacing s_t is defined similarly.

2.1.2 Safety factors at cracks

The governing equations of the MCFT are expressed in terms of mean stresses and strains. Therefore, it is necessary to check that the reinforcement is adequate to maintain equilibrium at cracks as illustrated in Figs. 4(a)-(c). The crack normal stress f_{ci} in Fig. 4(c) is assumed to be zero in the current version of the MCFT (Collins *et al.* 2008). The maximum stresses in the reinforcement f_{slcr} and f_{stcr} are given by Eqs. (4)-(5) of the MCFT (see Table 1) which are indeterminate to one degree since the crack shear stress v_{ci} is unknown. Therefore, it is only possible to check whether or not the stresses f_{slcr}, f_{stcr} and v_{ci} are within their permissible range. For this purpose, the maximum reinforcement stresses are initially calculated with $v_{ci} = 0$. The crack shear stress v_{ci} is only invoked if the reinforcement is overstressed in one direction. In this case, v_{ci} is found from equilibrium assuming that the stress in the critical reinforcement direction equals its maximum permissible value. The element is safe if $|v_{ci}| \le v_{ci,per}$ and the reinforcement stress is within its permitted range in the other direction. The safety factor at the crack is defined as $SF = Min\left(\left|\frac{f_{slcr,per}}{f_{slcr}}\right|, \left|\frac{f_{stcr,per}}{f_{stcr}}\right|\right)$ when $v_{ci} = 0$ or the reinforcement is overstressed in both directions.

$SF = \dfrac{v_{ci,per}}{|v_{ci}|}$ when $v_{ci} \neq 0$ and the least stressed reinforcement is not overstressed.

3. Reinforcement design

This paper considers two alternative strategies for designing the reinforcement in the HB and VB which are designated A and B. Strategy A sets the reinforcement ratio in each VB or HB equal to the greatest of the ratios required in any of its linked VHB bunches. Strategy B seeks to reduce the

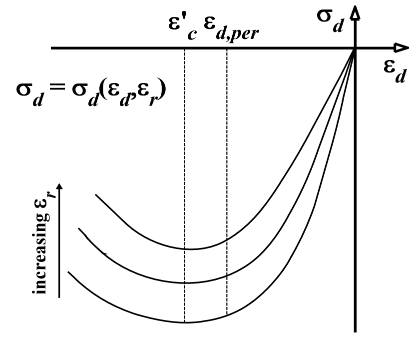

Fig. 2 Definition of maximum permissible concrete compressive strain

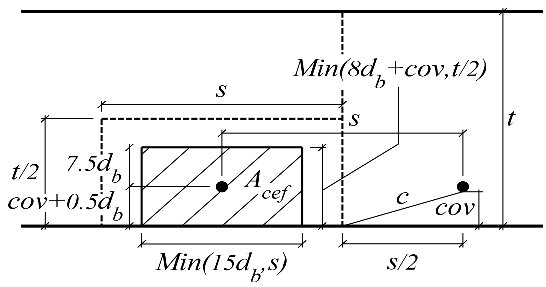

Fig. 3 Effective concrete area used in calculation of crack spacing

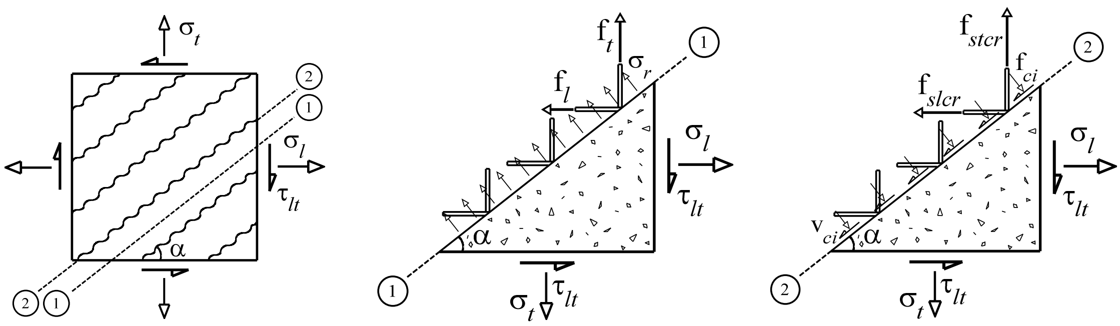

(a) applied stresses (b) average stresses (c) local stresses at a crack

Fig. 4 Average and local stresses

reinforcement weight below that given by strategy A by taking account of the linkage between the reinforcement in the VHB. In each case, the reinforcement is initially designed to resist the stresses from a linear FEA. Subsequently, the reinforcement is redesigned using stresses calculated in a NLFEA with the updated reinforcement. This procedure is repeated until the convergence criterion in Section 3.3 is satisfied.

3.1 Reinforcement design in individual VHB (Strategy A)

NonOpt uses a direct search procedure to find the minimum sum of the reinforcement ratios, ($\rho_{total} = \rho_l + \rho_t$), that is required to satisfy the design constraints at every Gauss point in each VHB. The final reinforcement in each HB and VB is taken as the greatest of the ratios in the linked VHB. The first step in the reinforcement design is to generate an equally spaced mesh in the $\rho_l - \rho_t$ plane between the minimum and maximum permitted reinforcement ratios, ρ_{min} and ρ_{max}, as depicted in Fig. 5. The solution procedure involves moving sequentially through the mesh on parallel lines defined by: $2\rho_{min} \leq \Lambda_i = \rho_{li} + \rho_{ti} \leq 2\rho_{max}$. The design constraints are checked at every Gauss point in the VHB at successive coordinates on parallel lines Λ_i until a solution is found. This involves firstly solving the rotating crack equations of the MCFT with the current applied stresses and reinforcement ratios and then checking the design constraints. The current reinforcement combination is declared invalid and updated as soon as a design constraint is violated.

This procedure is continued until a reinforcement combination, (ρ_l , ρ_t), is found which satisfies the design constraints at every Gauss point in the VHB cell. The subsequent movement on the reinforcement mesh depends on the specified number of mesh refinements, n_r. If n_r is greater than zero, the mesh is refined between the parallel line passing through the solution and the adjacent parallel line with δ_ρ less total reinforcement as shown in Fig. 5. The incremental step is taken as δ_ρ/n_d in the refined mesh. Each coordinate is checked in the refined mesh until a solution is found. Subsequently, the mesh is refined again if required and the preceding steps are repeated until the number of mesh refinements equals its specified value. Otherwise, the computations are continued along the current parallel line beyond the initial solution as there may be other points on the line

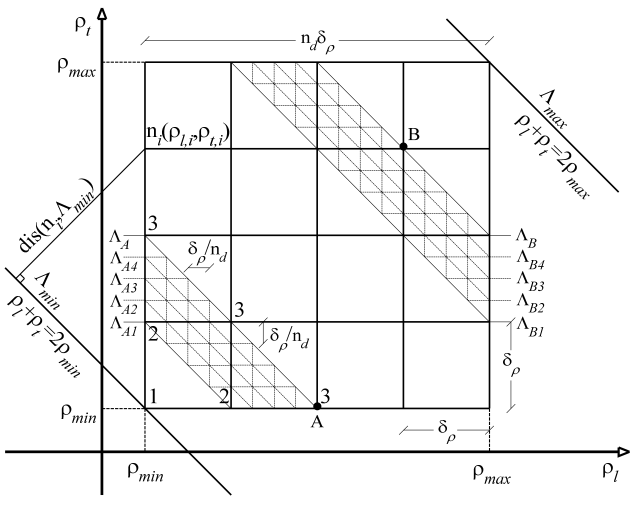

Fig. 5 Mesh generation and refinement (2D)

which satisfy all the design constraints. The final solution is taken as that with the greatest safety factor (*SF*) in cases where multiple solutions exist with the same value of ρ_{total}. The reinforcement in each VB and HB is taken as the greatest of the ratios required in its linked VHB.

3.2 Optimised reinforcement design with Strategy B

Consideration of strategy A shows that it can result in the provision of surplus reinforcement since no account is taken of the linkage between the reinforcement in the VHB. Strategy B seeks to account for this linkage by minimising the sum of the reinforcement ratios in up to four linked VHB which are selected on the basis of their relative safety factors as described below.

Safety factors are initially calculated for each VHB, as described in Section 2.1, using the results from the current FEA. VHB are subsequently classified as either: 1- independent, 2- horizontally independent (H-free) or vertically independent (V-free) bunches or 3- dependent as described below. The reinforcement is fully defined throughout the structure once the reinforcement ratios have been determined in the independent and -free bunches. The VHB are classified sequentially starting from the VHB with the lowest safety factor which is defined as the first independent bunch. The remaining VHB are checked in order of ascending safety factor to determine their classification. VHB are classified as independent if their reinforcement is not defined in either direction by that in previously defined independent VHB. Bunches are defined as dependent if their reinforcement is fully defined by that in independent bunches. H-free and V-free bunches are linked to an independent VHB in the non free direction. Unlinked bunches are

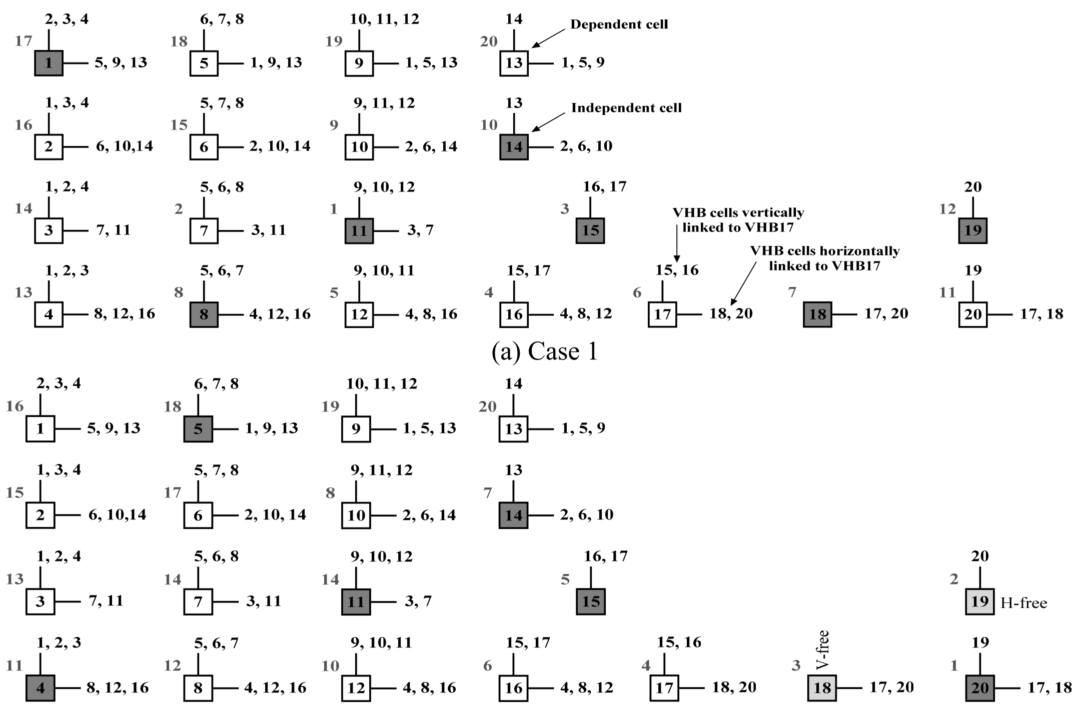

(a) Case 1

(b) Case 2

Fig. 6 Classification of VHB bunches

independent in the sense that their reinforcement ratios are unconstrained by any other idependent bunches.

This procedure is illustrated in Fig. 6 for the deep beam shown in Fig. 1 which is divided into 26 VHB. The VHB form two independent groups, namely VHB1 to 20 and VHB21 to 26, which are not linked in any direction. Figs. 6(a)-(b) show the linkage between VHB1 to 20 for two separate scenarios. The VHB number is shown at the centre of each bunch. Dark grey shading is used to depict independent bunches and light grey to depict H-free and V-free bunches. White squares depict dependent VHB bunches. The number at the top left hand corner of each VHB depicts its relative safety factor with one being least safe. The numbers adjacent to the horizontal and vertical markers depict the linked VHB bunches in the horizontal and vertical directions respectively.

VHB11 is the first independent bunch in Fig. 6(a) as it has the lowest safety factor (SF). VHB7 has the next lowest safety factor but is not independent as it is linked to VHB11. Therefore, VHB15 which has a relative safety factor of 3 is the second independent bunch as it is not linked to VHB11. The remaining bunches in Fig. 6(a) are checked similarly to find the other independent bunches which are VHB11, 15, 18, 8, 14, 19 and 1 in ascending order of safety factor with 11 being the least safe. The results of a similar procedure are shown in Fig. 6(b) for Case 2 where VHB18 and VHB19 are V-free and H-free respectively since the reinforcement is only defined by an independent VHB in one direction.

3.2.1 Reinforcement design in strategy B

The reinforcement is designed in the sequence indicated in the flowchart shown in Fig. 7. The first step is to design the reinforcement in the independent VHB using the procedure described in Section 3.1. Subsequently, the reinforcement is updated in the HB and VB and the safety factors are recalculated in the predefined dependent VHB to determine whether any of their safety factors are less than one. If so the VHB with the lowest overall safety factor is defined as critical. The reinforcement is subsequently redesigned in the two independent VHB linked to the critical dependent VHB subject to the constraint that the safety factors are greater than one in their one or two linked dependent VHB. For example, consider VHB4 in Fig. 6(a) to be the most critical dependent VHB. Its two linked independent bunches are VHB1 and VHB8. Fig. 6(a) shows that VHB1 and VHB8 are also linked to VHB5 which is dependent. Therefore, the design procedure would minimise the sum of the reinforcement ratios in VHB1 and VHB8 subject to the requirement that the design constraints are satisfied at every Gauss point in VHB1, VHB4, VHB5 and VHB8. Subsequently, the reinforcement is updated and the procedure is repeated until there are no critical dependent VHB.

The next step is to identify whether there are any H-free and V-free bunches with safety factors less than one. If so, the H-free (or V-free) bunch with the lowest safety factor is defined as critical. Its reinforcement is defined in one direction by an independent VHB but is free in the other direction. Consider for example that VHB19 in Fig. 6(b) is a critical H-free bunch. Its linked independent bunch is VHB20. The reinforcement in these two VHB is fully defined by three independent ratios (ρ_l and ρ_t in VHB20 and ρ_l in the VHB19). The sum of these three ratios is minimised subject to the constraint that the safety factors are greater than one in VHB19 and VHB20. NonOpt considers all the H-free bunches before moving on to the V-free bunches which are dealt with similarly.

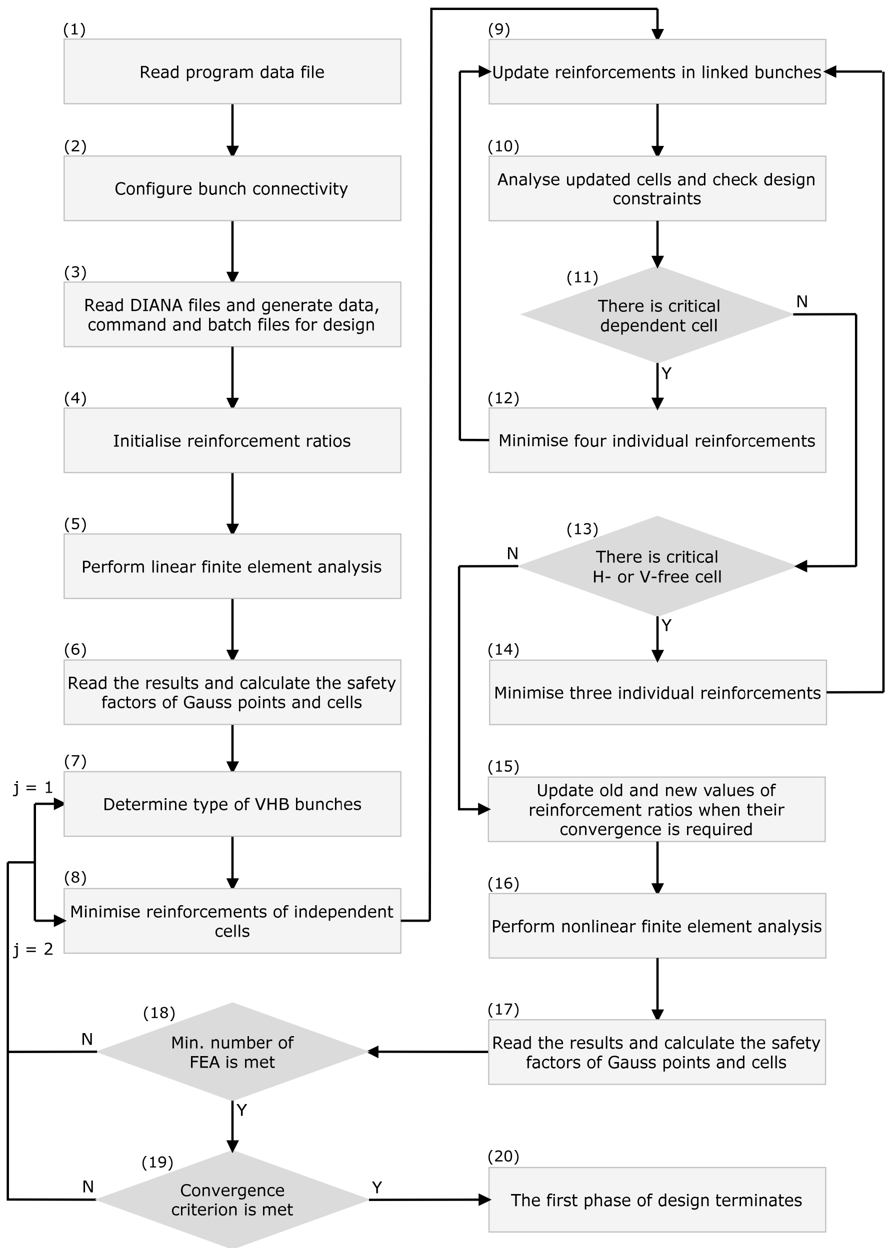

Fig. 7 Flowchart of design strategy B

3.2.2 Reinforcement optimisation in linked VHB

The reinforcement is designed in linked bunches using a similar procedure to that described in Section 3.1 for individual VHB. The key difference is that the sum of three or four independent reinforcement ratios is minimized compared with the sum of two ratios for individual VHB. The objective is to minimize the sum of three or four individual reinforcement ratios whilst satisfying the design constraints in the linked VHB whose reinforcement ratios are fully defined by the reinforcement being minimized.

The first step in the minimization of three independent reinforcement ratios is to generate an equally spaced 3D reinforcement mesh. The axes depict ρ_l and ρ_t in the independent VHB and the free reinforcement ratio in the H-free (ρ_l) or V-free (ρ_t) bunch. The permissible reinforcement ratios ($\rho_{\min}$ and $\rho_{\max}$) and mesh divisions (n_d) are the same as used in the 2D mesh. In a 3D mesh, any constant value of $\rho_{total} = \sum_{i=1}^{3} \rho_i$ represents a plane (see Fig. 8). Varying ρ_{total} from $3\rho_{\min}$ to $3\rho_{\max}$ in increments of δ_ρ covers the permissible domain in parallel planes. The movement starts from coordinate 1 at which $\rho_{total} = 3\rho_{\min}$ and moves sequentially in and between parallel planes in which $\rho_{total} = \sum_{i=1}^{3} \rho_i$. The design constraints are checked with the current reinforcement ratios at every Gauss point in the linked VHB within which the reinforcement is fully defined by the three reinforcement ratios being minimized. The checking of the design constraints requires the solution of the equations of the MCFT at each Gauss point. The current reinforcement combination is declared invalid and updated as soon as a design constraint is violated. This process is continued until a solution (i.e., a reinforcement combination) is found at which point the reinforcement mesh is either refined between the current and previous planes in the reinforcement mesh or a search is made for other solutions with the same ρ_{total}. The final solution is taken as that with the greatest safety factor (*SF*) in cases where multiple solutions exist with the same value of ρ_{total}.

The minimization of four individual reinforcements is done similarly with the only difference being that a 4D reinforcement space is used. For each critical dependent bunch, a 4D mesh is generated that incorporates the four reinforcement ratios in the two linked independent bunches. Each coordinate in the 4D mesh fully defines the reinforcement in the three or four linked VHB being considered in the minimization procedure. Varying ρ_{total} from $4\rho_{\min}$ to $4\rho_{\max}$ in increments of δ_δ covers the permissible domain in parallel hyperplanes in which $\rho_{total} = \sum_{i=1}^{4} \rho_i$ is constant. The movement starts from coordinate 1 at which $\rho_{total} = 4\rho_{\min}$ and moves sequentially in and between parallel hyperplanes in which ρ_{total} is constant. The direction of movement is from $4\rho_{\min}$ to $4\rho_{\max}$. The design constraints are checked with the reinforcement ratios corresponding to each coordinate in the 4D mesh until a solution is found. This involves solving the equations of the MCFT and calculating the safety factors at successive Gauss points in the three or four linked VHB for the current reinforcement combination. The safety factor of the group of linked bunches involved in the minimization is defined as the least of the safety factors of the individual VHB. The design procedure moves to the next coordinate in the hyperplane as soon as a design constraint is violated. This procedure is continued until a solution is found at which point the reinforcement mesh is either refined between the last two parallel hyperplanes or a search is made for other solutions with the same ρ_{total}. The final solution is taken as that with the greatest safety factor in cases where multiple solutions exist with the same value of ρ_{total}.

All coordinates in the reinforcement mesh are admissible during the initial minimization of the reinforcement in the independent VHB (box 8 in Fig. 7) which is performed after each FEA but the current reinforcement ratios are taken as the starting point in subsequent minimizations of the sum of three or four individual reinforcements in boxes 12 and 14 of Fig. 7. The sum of the reinforcement ratios in any independent, H-free or V-free bunch is prevented from reducing in the minimization procedure to avoid the possibility of the design procedure becoming stuck in anendless loop. Coordinates are only permitted in the 2D virtual reinforcement grid that defines thereinforcement in the independent, H-free or V-free VHB under consideration if

$\rho_l^{new} + \rho_t^{new} \geq \rho_l^{old} + \rho_t^{old}$ (where new refers to the current minimization and old the previous). For cases in which $\rho_l^{new} + \rho_t^{new} = \rho_l^{old} + \rho_t^{old}$, the validity of a coordinate can only be determined by comparing the new and old reinforcement coordinates (e.g., ρ_l^{old} and ρ_l^{new}). The second point on the current parallel line in the virtual reinforcement grid is always valid but the third is only valid if the direction of movement is away from the first point as illustrated in Fig. 9 in which the coordinates of the first and second points on a line are shown with circles. Valid and invalid coordinates for the next movement are depicted with ticks and crosses respectively.

3.3 Convergence criteria

The design can be safely terminated when the design constraints are first satisfied at every Gauss point in the structure. However, it is possible that the reinforcement ratios can be further minimized since the reinforcement is designed using stresses calculated in a NLFEA with the previous reinforcement arrangement. Consequently NonOpt gives the user two options, which are depicted C1 and C2, for continuing the reinforcement design procedure after the design constraints are first satisfied.

In option C1, the user specifies a minimum number of FEA in addition to the design constraints. The design terminates when the design constraints are satisfied at every Gauss point following a

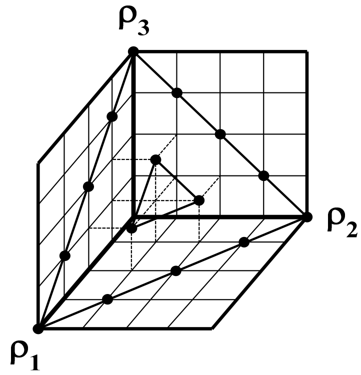

Fig. 8 Coordinates in a plane with constant value of ρ_{total} in a 3D mesh

(a) first point on parallel line (b) second point on parallel line

Fig. 9 Valid and invalid points in terms of moving direction

NLFEA with the current reinforcement arrangement and at least the specified minimum number of FEA have been completed. The number of reinforcement design iterations is one less than the total number of FEA as a NLFEA is carried out after every reinforcement design. For example, the reinforcement is designed for the elastic stress field if two FEA are specified. Option C2 requires the reinforcement ratios to converge within a prescribed tolerance. In this case, the design terminates if the design constraints are met and the reinforcement ratios have converged in successive iterations.

4. Case study of a deep beam with opening

A case study of the deep beam in Fig. 10 is presented to demonstrate the effectiveness of the proposed design procedure. The beam has been previously designed by Schlaich *et al*. (1987) using a simplified STM as well as Fernández Ruiz and Muttoni (2007) using the NLFEA procedure described in Section 1. The NLFEA was carried out with DIANA (2007) using its total strain rotating crack model in conjunction with the material properties described below. Comparisons are drawn between the reinforcement ratios and weights given by strategies A and B as well as those reported in the literature (Schlaich *et al*. 1987, Fernández Ruiz and Muttoni 2007). The designs are carried out with sub-strategy B_1 in which the VHB bunches are classified as independent, H-free, V-free or dependent after each FEA (j = 1 in box 7 of Fig. 7), using the constitutive relationships and design constraints described below.

4.1 Material properties and constitutive relationships

The concrete compressive strength is taken as 30 MPa with $\varepsilon_c' = -0.002$. The concrete compressive behaviour is modelled in accordance with the recommendations of Collins and Porasz (1989)

$$\sigma_d = -\beta f_c' \frac{m\left(\frac{\varepsilon_d}{\varepsilon_c'}\right)}{(m-1) + \left(\frac{\varepsilon_d}{\varepsilon_c'}\right)^{mk}} \tag{18}$$

in which

$$m = 0.8 + \frac{f_c'}{17} \quad (MPa) \tag{19}$$

$$k = 1; \quad \varepsilon_c' < \varepsilon_d < 0 \tag{20}$$

$$k = 0.67 + \frac{\beta f_c'}{62} \quad (MPa); \quad \varepsilon_d \le \varepsilon_c' \tag{21}$$

$$\beta = \frac{1}{1 + k_c} \le 1 \tag{22}$$

$$k_c = 0.27\left(-\tfrac{\varepsilon_r}{\varepsilon_c'} - 0.37\right) \tag{23}$$

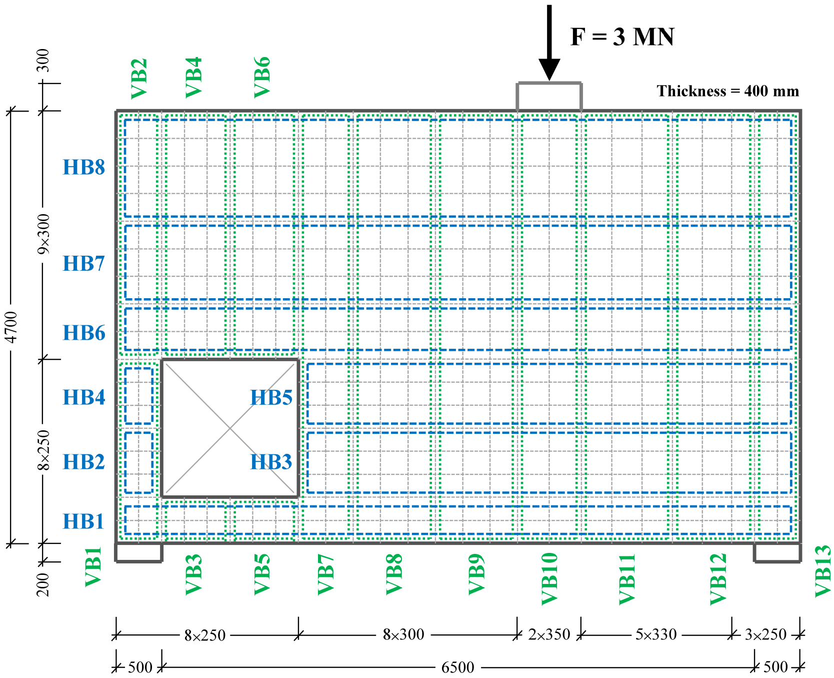

(a) bunch arrangement BA1

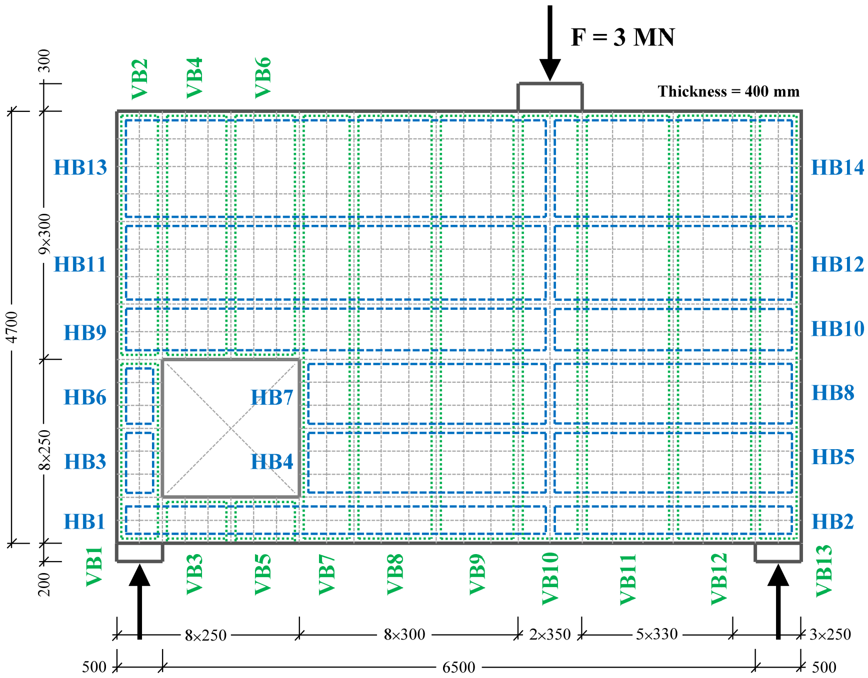

(b) bunch arrangement BA2

Fig. 10 Deep beam with opening

The concrete tensile strength is taken as $f_{cr} = 0.33\sqrt{f_c'}$ as recommended by Vecchio and Collins (1986) as is the response after cracking which is modeled as follows

$$\sigma_r = \frac{f_{cr}}{1+\sqrt{200\varepsilon_r}} \tag{24}$$

The stress-strain response of the reinforcement is modeled as bilinear with an elastic modulus of 200 GPa. The yield strength is taken as 500 MPa which corresponds to a yield strain of ε_y = 0.0025. The post-yield tangent modulus is taken as $E_s' = 0.842$ GPa with a characteristic strain at the maximum force equal to 0.05 which complies with Ductility Class B in EC2 (BSI 2004). Steel bearing plates are modeled elastically with an elastic modulus of 200 GPa and a Poisson's ratio of $\nu = 0.3$.

4.2 Design constraints

No restrictions are placed on the maximum principal tensile strain in the concrete or the mean strain in the reinforcement as the case studies only consider the ULS. The permissible principal compressive strain in the concrete is taken as $|\varepsilon_{d,per}| = 0.0017$ which is 85% of the strain at the peak stress. The maximum permissible reinforcement stress at cracks is limited to $f_{slcr,per} = f_{stcr,per}$ = 536MPa which is the stress at 90% of the assumed strain at the maximum force. The crack spacing is calculated automatically in the maximum stress computations in which the concrete cover, bar spacing and maximum aggregate size are assumed to be 25, 200 and 20 mm respectively. The number of reinforcement mesh divisions is taken as $n_d = 10$ ($\delta_\rho = 0.0038$) without any refinement ($n_r = 0$). The permissible reinforcement ratios are taken as $\rho_{\min} = 0.002$ and $\rho_{\max} = 0.04$ in accordance with the requirements of Eurocode 2 (BSI 2004) for walls and columns. Convergence criterion C2 was used with $er_{bar} = (\rho_{new} - \rho_{old}) / \rho_{new} = 0.01$.

4.3 Results

The reinforcement was designed using bunch arrangements BA1 and BA2 in Fig. 10. Table 2 lists the initial and final reinforcement ratios and weights given by strategies A and B as well as those corresponding to the STM of Schlaich *et al*. (1987) and the NLFEA design procedure of Fernández Ruiz and Muttoni (2007). The initial reinforcement weights in Table 2 are calculated for the elastic stress distribution. The agreement between the initial reinforcement weights for Strategies A and B is coincidental and will not generally be the case. The final weights are significantly less than the initial weights due to the redistribution of stress which occurs due to material nonlinearity. Consideration of Table 2 shows that strategy B gives marginally lower final reinforcement weights than strategy A but the greatest reduction in reinforcement weight is achieved by refining the bunch arrangement. The reinforcement weight given by strategy B for BA2 is similar to but slightly greater than that calculated by Fernández Ruiz and Muttoni (2007). The reinforcement weights in Table 2 can be reduced by either increasing the number of reinforcement mesh divisions n_d or using mesh refinement ($n_r \geq 1$). The difference in reinforcement weights given by NonOpt and Fernández Ruiz and Muttoni (2007) is also a function of the different design constraints and constitutive relationships adopted in each approach. The inclusion of tension stiffening in NonOpt has a variable effect on the reinforcement weight. It tends to increase the reinforcement weight in beams with low amounts of web reinforcement as a result of a reduction in the proportion of load being directly transmitted to the supports through the concrete acting in compression. In other cases, the reinforcement weight can reduce due to the increase in concrete compressive strength resulting from the reduction in principal tensile strain. Fig. 11 shows the final reinforcement arrangement for BA2 along with the directions of the minimum principal strains.

Table 2 Reinforcement ratios and weights in deep beam with opening (TS = 1, n_d = 10 & n_r = 0)

	BA1				***BA2***				***BA1***	***BA2***
Strategy	*A*		*B*		*A*		*B*		*Fernán-dez Ruiz and Muttoni*	*Schlaich et al. STM*#
Results	***Initial***	***Final***	***Initial***	***Final***	***Initial***	***Final***	***Initial***	***Final***		
HB1	*0.0134*	*0.0096*	*0.0134*	*0.0096*	*0.0134*	*0.0096*	*0.0134*	*0.0096*	*0.0098*	*0.0063*
HB2	*0.0058*	*0.0020*	*0.0058*	*0.0058*	*0.0096*	*0.0058*	*0.0096*	*0.0058*	*0.0020*	*0.0020*
HB3	*0.0058*	*0.0058*	*0.0058*	*0.0058*	*0.0058*	*0.0020*	*0.0058*	*0.0058*	*0.0020*	*0.0023*
HB4	*0.0020*	*0.0020*	*0.0020*	*0.0020*	*0.0058*	*0.0058*	*0.0058*	*0.0020*	*0.0020*	*0.0020*
HB5	*0.0134*	*0.0058*	*0.0134*	*0.0020*	*0.0058*	*0.0058*	*0.0058*	*0.0058*	*0.0020*	*0.0023*
HB6	*0.0210*	*0.0096*	*0.0210*	*0.0058*	*0.0020*	*0.0020*	*0.0020*	*0.0020*	*0.0082*	*0.0117*
HB7	*0.0020*	*0.0058*	*0.0020*	*0.0058*	*0.0134*	*0.0058*	*0.0134*	*0.0020*	*0.0020*	*0.0020*
HB8	*0.0020*	*0.0020*	*0.0020*	*0.0020*	*0.0020*	*0.0020*	*0.0020*	*0.0020*	*0.0020*	*0.0020*
HB9	-	-	-	-	*0.0210*	*0.0096*	*0.0210*	*0.0058*	-	-
HB10	-	-	-	-	*0.0020*	*0.0020*	*0.0020*	*0.0020*	-	-
HB11	-	-	-	-	*0.0020*	*0.0058*	*0.0020*	*0.0058*	-	-
HB12	-	-	-	-	*0.0020*	*0.0020*	*0.0020*	*0.0020*	-	-
HB13	-	-	-	-	*0.0020*	*0.0020*	*0.0020*	*0.0020*	-	-
HB14	-	-	-	-	*0.0020*	*0.0020*	*0.0020*	*0.0020*	-	-
VB1	*0.0020*	*0.0020*	*0.0020*	*0.0020*	*0.0020*	*0.0020*	*0.0020*	*0.0020*	*0.0020*	*0.0020*
VB2	*0.0020*	*0.0020*	*0.0020*	*0.0020*	*0.0020*	*0.0020*	*0.0020*	*0.0020*	*0.0020*	*0.0020*
VB3	*0.0020*	*0.0020*	*0.0020*	*0.0020*	*0.0020*	*0.0020*	*0.0020*	*0.0020*	*0.0020*	*0.0020*
VB4	*0.0020*	*0.0020*	*0.0020*	*0.0020*	*0.0020*	*0.0020*	*0.0020*	*0.0020*	*0.0020*	*0.0023*
VB5	*0.0020*	*0.0020*	*0.0020*	*0.0020*	*0.0020*	*0.0020*	*0.0020*	*0.0020*	*0.0020*	*0.0020*
VB6	*0.0096*	*0.0020*	*0.0096*	*0.0058*	*0.0096*	*0.0020*	*0.0096*	*0.0058*	*0.0020*	*0.0023*
VB7	*0.0134*	*0.0096*	*0.0134*	*0.0096*	*0.0134*	*0.0096*	*0.0134*	*0.0096*	*0.0052*	*0.0117*
VB8	*0.0020*	*0.0020*	*0.0020*	*0.0020*	*0.0020*	*0.0020*	*0.0020*	*0.0020*	*0.0020*	*0.0020*
VB9	*0.0020*	*0.0020*	*0.0020*	*0.0020*	*0.0020*	*0.0020*	*0.0020*	*0.0020*	*0.0020*	*0.0020*
VB10	*0.0020*	*0.0020*	*0.0020*	*0.0020*	*0.0020*	*0.0020*	*0.0020*	*0.0020*	*0.0020*	*0.0020*
VB11	*0.0020*	*0.0020*	*0.0020*	*0.0020*	*0.0020*	*0.0020*	*0.0020*	*0.0020*	*0.0020*	*0.0020*
VB12	*0.0020*	*0.0020*	*0.0020*	*0.0020*	*0.0020*	*0.0020*	*0.0020*	*0.0020*	*0.0020*	*0.0020*
VB13	*0.0020*	*0.0020*	*0.0020*	*0.0020*	*0.0020*	*0.0020*	*0.0020*	*0.0020*	*0.0020*	*0.0020*
Sum	*0.1104*	*0.0762*	*0.1104*	*0.0762*	*0.1338*	*0.0958*	*0.1338*	*0.0920*	*0.0592*	*0.0669*
D*	-	-	-	-	-	-	-	-	-	*94*
Weight (kg)	*1168*	*858*	*1168*	*783*	*979*	*748*	*979*	*693*	*622*	*794*

*D denotes weight of diagonal bars in kg, # The reinforcement weight is calculated assuming that the ties in HB3 and HB5 are 5.5m long.

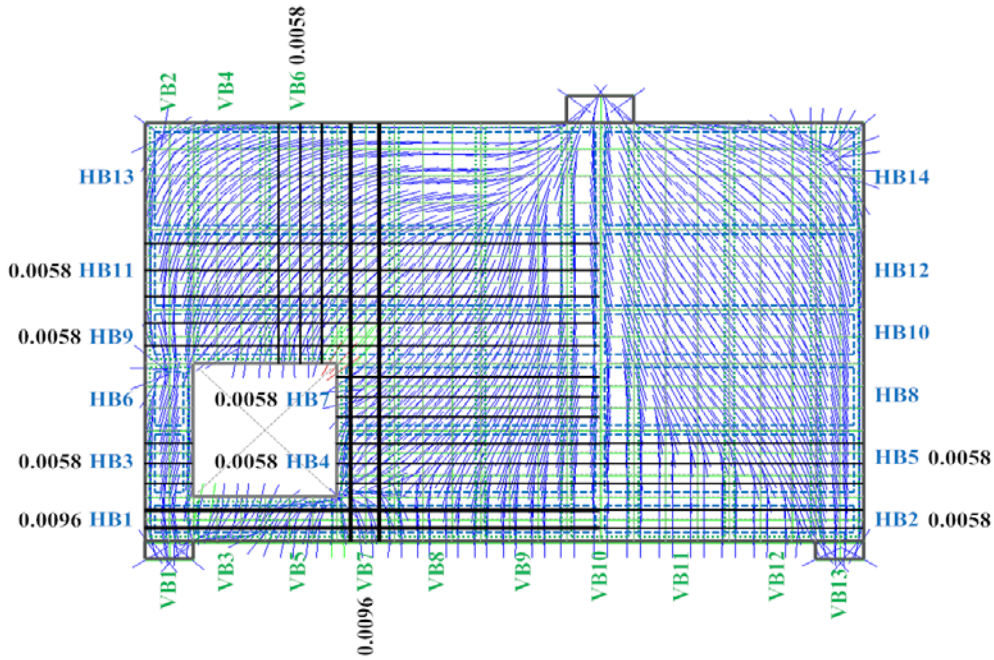

Fig. 11 Deep beam with opening: reinforcement ratios & directions of minimum principal strains for BA2

5. Conclusions

This paper proposes a practical nonlinear procedure for the semi-automated design of reinforced concrete structures subject to plane stress. The procedure incorporates nonlinear finite element analysis and is intended as an alternative to strut and tie modeling. The method is applicable to any reinforced concrete structure that can be modeled with plane stress elements but is intended for D regions in which plane sections do not remain plane.

The design procedure is implemented in NonOpt (Amini Najafian 2011) which is a FORTRAN program that works in conjunction with the finite element program DIANA (2007). The procedure is iterative due to the dependency of the finite element results on the reinforcement arrangement. The same constitutive relationships are used in the reinforcement design as well as the NLFEA to facilitate the satisfaction of the design constraints after a NLFEA with the final reinforcement arrangement. Practical reinforcement arrangements are achieved by grouping the elements of the finite element model into horizontal and vertical bands. This paper considers two alternative procedures for designing the reinforcement in a complete structure which are designated A and B. Strategy A sets the reinforcement ratio in each VB or HB equal to the maximum of the ratios required in the linked VHB bunches. Strategy B simultaneously minimizes the sum of three or four individual reinforcement ratios in linked groups from which the reinforcement in the entire structure is determined. The sum of the reinforcement ratios is minimized subject to design constraints which are chosen to ensure satisfactory structural performance. The case study demonstrates that the proposed procedure is a practical alternative to STM for the design of planar reinforced concrete structures. Strategy B is shown to be marginally more efficient than strategy A for the case studies considered but Strategy A is adequate for practical use. The final reinforcement weight depends on the bunching arrangement and can be reduced by refining the dimensions of the horizontal and vertical reinforcement bands around stress concentrations. Future work will consider the automation of the dimensioning of the reinforcement bands as this has a significant influence on the reinforcement weight.

References

ACI Committee 318 (2011), *Building code requirements for structural concrete and commentary*, ACI 318-11 and ACI 318R-11, American Concrete Institute, Farmington Hills, Michigan.

ACI-ASCE (2010), Joint ACI-ASCE Committee 445, SP-273, *Further Examples for the Design of Structural Concrete with Strut-and-Tie Models*, American Concrete Institute, Farmington Hills, Michigan.

Amini Najafian, H. (2011), "Nonlinear optimisation of reinforcement design for reinforced concrete structures loaded in plane stress", PhD Thesis, Department of Civil and Environmental Engineering, Imperial College London.

Bentz, E.C. (2000), "Sectional analysis of reinforced concrete members", PhD Thesis, Department of Civil Engineering, University of Toronto.

BSI (2004), European Standard EN-1992-1-1:2004, *Eurocode 2: Design of Concrete Structures, Part 1, General Rules and Rules for Buildings*, British Standard Institution, London.

Collins, M.P. and Porasz, A. (1989), "Shear design for high-strength concrete", *Comité Euro-International du Béton, Bulletin d'Information*, 193, 77-83.

Collins, M.P., Bentz, E.C., Sherwood, E.G. and Xie, L. (2008), "An adequate theory for the shear strength of reinforced concrete structures", *Mag. Concr. Res., 60,* 635-650.

CSA (2004), *Design of Concrete Structures,* CSA Standard A23.3-04, Canadian Standards Association, Ottawa.

DIANA (2007), *Finite Element Analysis User's Manual*, Release 9.2, TNO DIANA BV, Delft, The Netherlands.

Fernández Ruiz, M. and Muttoni, A. (2007), "On development of suitable stress fields", *ACI Struct. J.,* **104**, 495-502.

Fib (2011), *Design examples for strut-and-tie models,* fib Bulletin No. 61. fib, Lausanne, Switzerland.

Hong, S.G., Hong, N.K. and Jang, S.K. (2011), "Deformation capacity of structural concrete in disturbed regions", *ACI Struct. J.,* **108**(3), 267-276.

Hsu, T.C. (1993), *Unified Theory of Reinforced Concrete,* CRC Press Inc., Boca Raton, Florida, USA.

Kuchma, D., Yindeesuk, S. and Tjhin, T. (2010), "Large propped cantilever beam with opening, In. SP-273, Further examples for the design of structural concrete with strut-and-tie models", *ACI*, Farmington Hills, Michigan.

Kwak, H.G. and Noh, S.H. (2006), "Determination of strut-and-tie models using evolutionary structural optimization", *Eng. Struct.,* **28**(10), 1440-1449.

Park, J.W., Yindeesuk, S., Tjhin, T.N. and Kuchma, D.A. (2010), "Automated finite element validation of complex regions designed by the strut-and-tie method", *ASCE J. Struct. Eng.,* **136**(2), 203-210.

Perera, R. and Vique, J. (2009), "Strut-and-tie modelling of reinforced concrete beams using genetic algorithms optimization", *Const. Build. Mater.,* **23**, 2914-2925.

Schlaich, J., Schäfer, K. and Jennewein, M. (1987), "Toward a consistent design of structural concrete", *Prestressed Conc. Inst. J.*, **32**(3), 75-150

Tabatabai, S.M.R. (1996), "Finite element-based elasto-plastic optimum reinforcement dimensioning of spatial concrete panel structures", Doctoral dissertation, Institute of Structural Engineering, Swiss Federal Institute of Technology (ETH Zurich), also published by BirkhaÈuser Verlag, Basel.

Tabatabai, S.M.R. and Mosalam, K.M. (2001), "Computational platform for non-linear analysis/ optimal design of reinforced concrete structures", *Eng. Comput.,* **18**, 726-744.

Tjhin, T.N. and Kuchma, D.A. (2002), "Computer-based tools for design by strut-and-tie method: advances

and challenges", *ACI Struct. J.*, **99**, 586-594.
Vecchio, F.J. (1990), "Reinforced concrete membrane element formulations", *ASCE J. Struct. Eng.*, **116**(3), 730-750.
Vecchio, F.J. and Collins, M.P. (1986), "The modified compression field theory for reinforced concrete elements subjected to shear", *ACI J.*, **83**, 219-231.

Notations

a	Maximum aggregate size
f_c'	Concrete cylinder strength
f_{cr}	Tensile strength of concrete
f_l	Average stress in longitudinal reinforcement
f_{slcr}	Maximum stress in longitudinal reinforcement at a crack
$f_{scr,per}$	Maximum permissible stress in reinforcement at a crack
f_{stcr}	Maximum stress at crack in transverse reinforcement
f_t	Average stress in transverse reinforcement
f_y	Yield strength of reinforcement
f_{yd}	Design yield strength of reinforcement
n_d	Number of reinforcement mesh divisions
n_r	Number of reinforcement mesh refinements
s	Reinforcement spacing
s_l	Mean crack spacing in pure longitudinal tension condition
s_{ma}	Mean inclined crack spacing
s_t	Mean crack spacing in pure transverse tension condition
v_{ci}	Local shear stress in concrete along crack
$v_{ci,per}$	Permissible local shear stress in concrete along crack
$v_{ci\max}$	Maximum local shear stress that crack is able to transfer
w	Crack width
$w_{\max}$	Maximum permissible crack width
A_s	Area of reinforcement bars
$A_{s\min}$	Minimum area of reinforcement for crack control
E_s	Elastic modulus of reinforcement
E_s'	Post yield tangent modulus of reinforcement
SF	Safety factor
α	Cracking angle
β	Softening coefficient
γ_{lt}	Shear strain in *l-t* coordinate
δ_ρ	Incremental step of reinforcement ratio
ε_{cr}	Cracking strain of concrete
ε_y	Yield strain of reinforcement
ε_c'	Strain corresponding to peak stress in concrete stress-strain curve
ε_d	Compressive principal strain in concrete
$\varepsilon_{d,per}$	Permissible compressive strain in concrete
ε_l	Normal strain in longitudinal direction (strain in longitudinal reinforcement)

ε_r	Tensile principal strain in concrete
$\varepsilon_{r,per}$	Permissible principal tensile strain in concrete
ε_t	Normal strain in transverse direction (strain in transverse reinforcement)
ρ_i	Reinforcement ratio number i
ρ_{free}	Free reinforcement ratio
ρ_l	Longitudinal reinforcement ratio
ρ_l^{new}	Longitudinal reinforcement ratio in the current minimization process
ρ_l^{old}	Longitudinal reinforcement ratio in the previous minimization process
$\rho_{l,i}$	Longitudinal reinforcement ratio at point i in reinforcement mesh
$\rho_{\max}$	Maximum permissible reinforcement ratio
$\rho_{\min}$	Minimum permissible reinforcement ratio
ρ_t	Transverse reinforcement ratio
ρ_t^{new}	Transverse reinforcement ratio in the current minimization process
ρ_t^{old}	Transverse reinforcement ratio in the previous minimization process
$\rho_{t,i}$	Transverse reinforcement ratio at point i in reinforcement mesh
ρ_{total}	Total reinforcement ratio
σ_d	Compressive principal stress in concrete
$\sigma_{d,\max}$	Peak stress in softened concrete stress-strain curve
σ_l	Normal stress in reinforced concrete element in longitudinal direction
σ_r	Tensile principal stress in concrete
σ_s	Reinforcement stress
σ_t	Normal stress in reinforced concrete element in transverse direction
τ_{lt}	Shear stress in reinforced concrete element